JOC The Journal of Organic Chemistry

Article

pubs.acs.org/joc

Does a Cyclopropane Ring Enhance the Electronic Communication in Dumbbell-Type C_{60} Dimers?

Andrea La Rosa,[†,⊥] Katalin Gillemot,[∥,⊥] Edmund Leary,*[,‡,§,⊥] Charalambos Evangeli,[§,⊥] María Teresa González,[‡] Salvatore Filippone,[†] Gabino Rubio-Bollinger,[§] Nicolás Agraït,[‡,§] Colin J. Lambert,[∥] and Nazario Martín*[,†,‡]

[†]Departamento de Química Orgánica, Facultad de Química, Universidad Complutense, E 28040 Madrid, Spain

[‡]IMDEA-Nanoscience, Campus de Cantoblanco, Calle Faraday 9, Ciudad Universitaria de Cantoblanco, 28049 Madrid, Spain

[§]Laboratorio de Bajas Temperaturas, Departamento de Física de la Materia Condensada Módulo 13, Universidad Autónoma de Madrid, E-28049 Madrid, Spain

[∥]Department of Physics, Lancaster University, Lancaster LA1 4YB, U.K.

Supporting Information

ABSTRACT: Two C_{60} dumbbell molecules have been synthesized containing either cyclopropane or pyrrolidine rings connecting two fullerenes to a central fluorene core. A combination of spectroscopic techniques reveals that the cyclopropane dumbbell possesses better electronic communication between the fullerenes and the fluorene. This observation is underpinned by DFT transport calculations, which show that the cyclopropane dumbbell gives a higher calculated single-molecule conductance, a result of an energetically lower-lying LUMO level that extends deeper into the backbone. This strengthens the idea that cyclopropane behaves as a quasi-double bond.

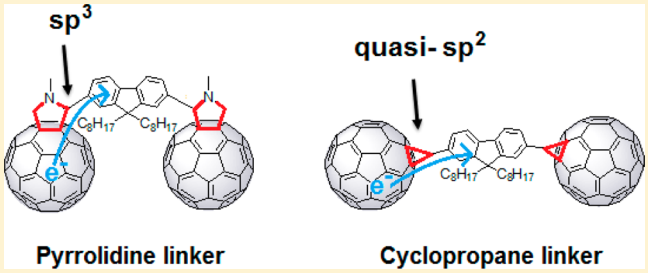

INTRODUCTION

The chemistry of fullerenes is well-established. Over the years, a wide variety of reactions have been carried out on the convex surface of [60]fullerenes, which have led to the incorporation of a wealth of organic functional groups covalently linked to the carbon framework.[1−3] Although most of the known reactions have been developed for improving their solubility and processability, a great number of these reactions have been focused on the chemical modification of the electronic properties of pristine C_{60}.[4,5] Thus, the inherent electron-acceptor features of C_{60} have often been modified in the search for fullerene derivatives exhibiting optimized redox properties for application in organic molecular electronics.[6−11]

Despite the interest in controlling the electronic communication between various organic addends and the fullerene sphere, no significant advances have, so far, been achieved. This can be attributed to the fact that addition of an addend across the fullerene double bond results in a saturated C−C bond, which forbids conjugation, preventing significant electronic communication between the two units. This leaves only inductive effects, which are typically responsible for the relatively weak influence that organic addends exert on the electronic properties of covalently connected fullerenes.[12] A few previous attempts have been carried out in the search for a covalently connected π-conjugated organic addend to the π-conjugated fullerene system. In this respect, Wudl and co-workers determined, by electrochemical methods, that "periconjugation" exists between an addend π-system and the fullerene unit, due to the overlap existing between the p_z orbitals of the addend with the perpendicularly oriented p_z orbitals of the fullerene double bonds.[13,14] This is, though, a very weak effect, being a consequence of the distance between the orbitals and their orthogonal positioning toward each other.[15]

More recently, Hummelen and co-workers carried out the preparation of, albeit synthetically highly demanding, [6,6] and [5,6] vinyl-substituted C_{60} in the search for new [5,6]-alkylidenehomofullerenes, in which the connectivity between the organic addend and the buckyball core takes place through alternating double and single C−C bonds. However, once again, the geometrical features of these systems prevent effective electronic communication between both π-systems.[16]

Only very recently, by fusing the π-electron system of C_{60} and an oligothiophene through an open-cage strategy, has the visible absorbance of fullerenes been significantly enhanced and their absorption pushed into the near-infrared (NIR) region. Although a relative control of the HOMO and LUMO energy levels is achieved, this skillful alternative for extending the conjugation beyond the carbon cage results in a breaking of the C_{60} π-electron system due to the presence of the hole in the fullerene sphere.[17]

Received: February 17, 2014
Published: April 21, 2014

 © 2014 American Chemical Society dx.doi.org/10.1021/jo500342x | J. Org. Chem. 2014, 79, 4871−4877

Scheme 1. Synthesis of Dumbbell-Type Molecules 4 and 6

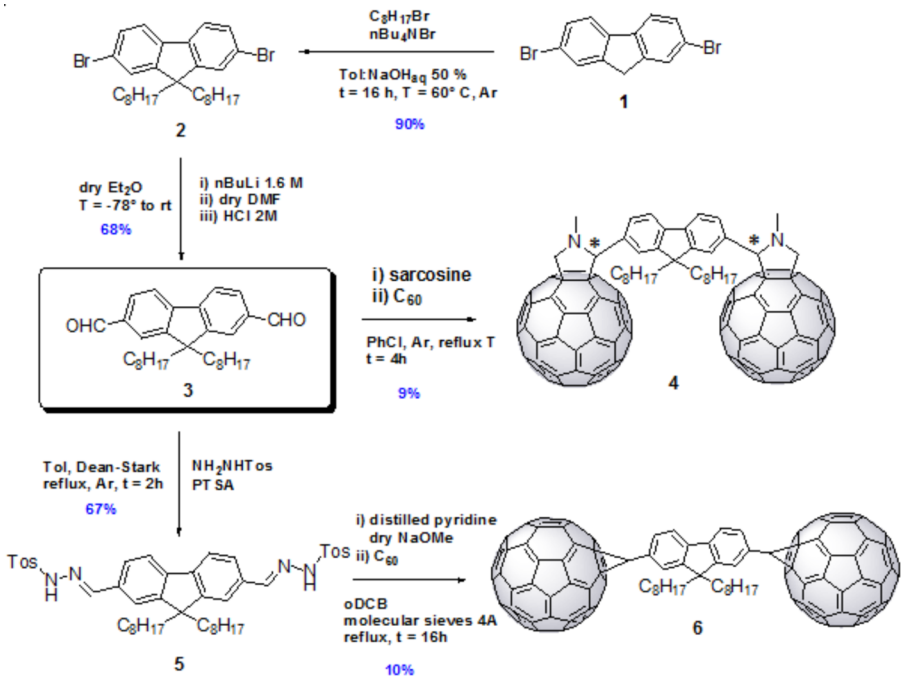

In light of the above results, and also motivated by our recent progress in wiring single molecules with C_{60} anchor groups,[18,19] we decided to examine two fullerene derivatives with different groups connecting a central fluorene (Fl) bridge to two C_{60} groups. Our idea was to investigate whether electronic communication could be enhanced by substituting pyrrolidine (Py) connecting groups for cyclopropane (Cp) groups. It is well-known that pristine Cp undergoes the typical reactivity of an olefin. This singular behavior can be accounted for by noting that the C−C bonding can be described through bent bonds, in which the electron density does not lie along the direct lines connecting the carbon nuclei.[20] Moreover, the bonding orbitals exhibit a comparatively high-lying energy for a saturated hydrocarbon giving the bonds considerable π character.[21]

Compound **6**, for which we have previously described the synthesis,[19] contains two Cp rings, each fused to a single C_{60} and joined through a single Fl bridge. To benchmark our results, we have prepared compound **4**, shown in Scheme 1, in which the C_{60}s are connected to the Fl through the completely saturated Py groups. Further experimental details are given in the Experimental Section and characterization data in the Supporting Information. The Py groups are expected to have reduced communication in comparison to the Cp groups due to their completely saturated bond characteristics. Initially, we employed detailed density functional calculations to assess the electronic structure and transport properties. Following this, we investigated the electronic properties of each compound using different spectroscopic tools, including cyclic voltammetry (CV) and UV−vis spectroscopy. We have also characterized both compounds using a scanning tunneling microscope (STM), which verified the dumbbell structure of both (see Figure 1). We attempted to measure the conductance between the two C_{60} groups of each compound between wired between the tip and the surface. The results of this study are shown in the Supporting Information.

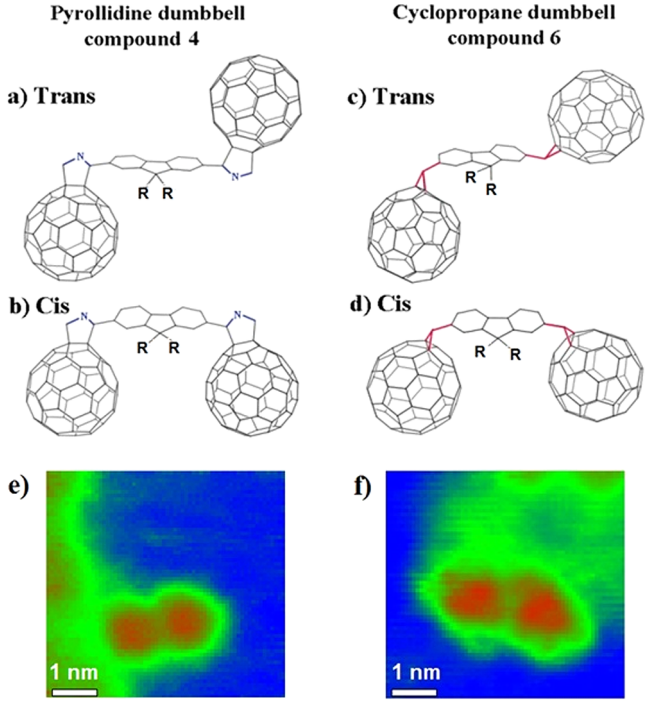

Figure 1. (a−d) Main conformational isomers of compounds **4** and **6** (R = C_6H_{13}). The calculated distance between the centers of the C_{60} cages are as follows: (a) 1.62 nm; (b) 1.27; (c) 1.64; (d) 1.56 nm. (e, f) Scanning tunneling microscopy (STM) images of **4** and **6** adsorbed to a gold (111) surface and imaged using a bias of 0.1 V. (e) STM image of compound **4**, which is adsorbed to a gold step through one C_{60}. The measured C_{60} center to center (c to c) distance is 1.2 nm, suggesting the cis conformation. (f) STM image of compound **6**, which is adsorbed to a gold step through both C_{60} groups. The measured c to c distance is 1.7 nm, suggesting the trans conformation.

dx.doi.org/10.1021/jo500342x | J. Org. Chem. 2014, 79, 4871−4877

RESULTS AND DISCUSSION

Comparing the structures of **4** and **6**, there are some important differences which merit consideration regarding optimal wire geometry. In both cases, there are at least two (formally) sp^3 carbon atoms separating the π conjugated Fl from the π system of the C_{60}, one (Py) or two (Cp) belonging to the fullerene core and one situated outside, joining the buckyball to the Fl. In both compounds, this leads to two main cis and trans conformers, which are shown in Figure 1 (a–d).

By depositing the compounds on gold (111) surfaces (see the Supporting Information for details) we have identified both isomeric forms. Figure 1e shows a scanning tunneling microscope (STM) image of compound **4**, in which the distance between the centers of the two C_{60} groups is measured to be 1.2 nm, suggesting the cis conformation. Figure 1f, on the other hand, shows an STM image of **6** in which the separation of the C_{60} groups is larger at 1.7 nm, fitting with the trans conformation. We can observe both conformations of **4** on the surface, although resolving the differnt conformers of **6** is more difficult due to a smaller difference in C_{60} separation. In the structure of molecule **4** the C-2 position of the Py ring is chiral (labeled with an asterisk in Scheme 1), as are the nitrogen atoms, forming a total of four stereogenic centers. This leads to many different stereoisomers of **4**, which combined with the freedom of rotation about the bond adjoining the Fl and the Py groups produces a large variety of potential geometries within a molecular junction. Molecule **6** has no such stereogenic centers and is also a much more rigid, symmetric, and linear molecule than **4**, making it a far better candidate as a molecular wire just considering its structural properties.

Theoretical Transport Calculations. To gain initial insight into the electronic structure of compounds **4** and **6**, and to assess their transport properties, we have carried out large-scale density functional theory calculations combined with Green's function based transport studies. In our models, the fully relaxed molecules (with a force tolerance of 0.02 eV/Å) were fitted between ⟨111⟩ oriented ideal gold electrodes. The relaxed geometry and the tight binding Hamiltonian of the system were acquired using the ab initio DFT package Siesta[22] in the local density approximation (LDA) with Caperley–Alder parametrization[23] and Troullier–Martins-type nonrelativistic, norm-conserving pseudopotentials,[24] using a double-ζ basis set and a real space grid of 200 Ry. Once the electronic structure was obtained, we used the SMEAGOL code[25,26] to calculate the electronic transport properties of the system. As we are interested in the low-bias voltage properties of these molecules, we used an "equilibrium" implementation, which calculates the zero-bias transmission coefficient $T(E)$ more efficiently for electrons of energy E passing through the molecule from one electrode to the other. The conductance is then obtained via the Landauer formula $G = (2e^2/h)T(E_F)$, where E_F is the Fermi level of the gold electrodes.

The electrodes were chosen flat to model the STM experiments, and the optimal distance between the leads and the molecules was found by minimizing the DFT energy of a single C_{60} next to a gold surface. This resulted in a distance of 0.23 nm, which agrees well with the results from Markussen et al.[27] For both compounds **4** and **6**, two conformational isomers were considered (labeled Cis and Trans, see Figure 1). Figure 2 shows the transmission coefficients $T(E)$ for both compounds **4** and **6** and a pristine C_{60} molecule for comparison. Both molecules conduct through their LUMO level, and we find

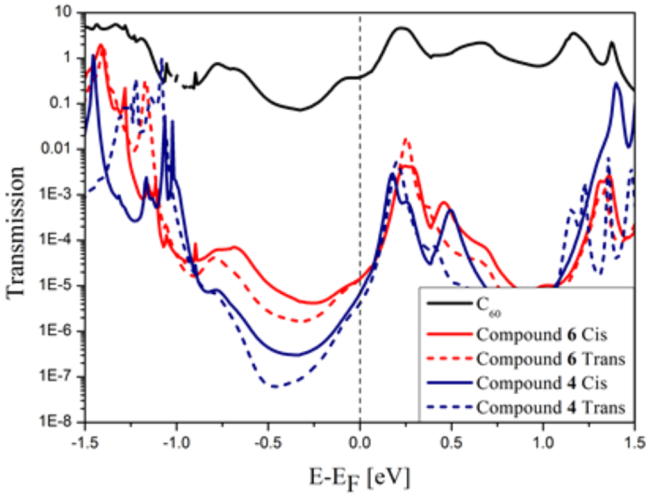

Figure 2. Transmission vs energy for both isomers of compounds **4** and **6** and for pristine C_{60}. The black dashed line indicates the Fermi energy.

that the conductance values follow the order C_{60} (0.4 G_0) ≫ cyclopropane dumbbell **6** (1.5×10^{-5} G_0) > pyrrolidine dumbbell **4** (6×10^{-6} G_0) at E_F, agreeing with the discussion of the previous section and our basic postulation of higher electronic coupling for **6**. It is well-known that DFT usually underpredicts the HOMO–LUMO gap, so it can be safely assumed that the conductance difference between compound **4** and **6** is at least a factor two, as the ratio would only increase if E_F moved further into the molecular HOMO–LUMO gap upon widening. The transmission at E_F along with the LUMO peak does not vary significantly between the cis and trans conformations of both compounds; however, there are larger differences near the resonance assigned to the HOMO of the system. This is likely to be associated with the first LUMO orbitals being localized on the C_{60}, while the HOMO extends throughout the Fl backbone, which moves more between the various conformations relative to the electrodes.

To understand the positioning and ordering of the energy levels of each system, we have projected the respective full Hamiltonian, comprising the molecules plus the leads, onto the subspace spanned by the basis functions of the molecules (yielding a Hamiltonian containing information only about the molecules) using the same procedure as explained by Markussen et al.[27] This is further detailed in the Supporting Information. This procedure takes into account the charge transfer from the metal onto the molecules. Looking at the calculated energy differences between the Fermi level and the LUMO levels in Figure 3, the general trend of all the LUMO levels is to increase in energy going between C_{60}, compound **6**, and compound **4**. There are some exceptions, presumably reflecting the fact that Kohn–Sham orbitals do not represent the molecular orbitals accurately enough and that the error is also larger for the higher lying LUMO levels. The trend in the position of the first LUMO level of compounds **4** and **6** is more obvious for the trans conformations, while being less clear for the cis case. It is also interesting to note that the splitting of the first LUMO pair is much less pronounced in **4** compared with **6**.

The lower lying LUMO level for compound **6** is consistent with the higher transmission at E_F found in Figure 2. The LUMO of compound **6** does not, however, approach the Fermi level as close as for pristine C_{60}, which is understandable since the level will be partially influenced by the Cp groups and the Fl.

dx.doi.org/10.1021/jo500342x | J. Org. Chem. 2014, 79, 4871–4877

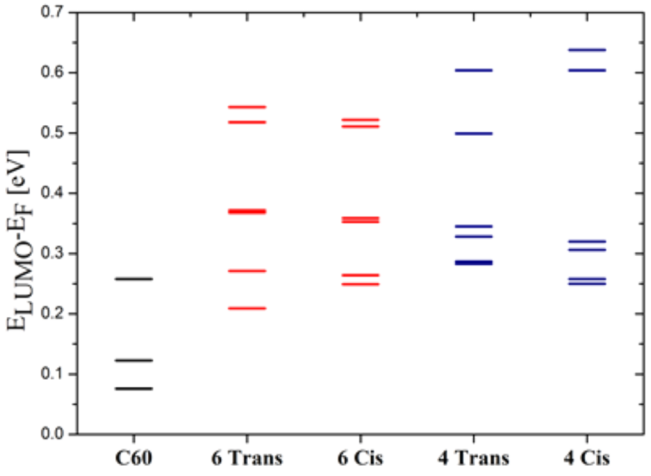

Figure 3. First three LUMO levels for C_{60} and the first six LUMO levels for compounds **4** and **6**. The thicker lines are levels close to each other.

Looking again at the transmission curves in Figure 2, the transmission of compound **6** clearly does not drop as significantly as **4** at the center of the HOMO−LUMO gap. A possible explanation for this is that, apart from lying at a lower energy, the first LUMO level is also better coupled through space. Considering that we expect the Cp groups to behave in a similar fashion to a double bond, we wanted to analyze whether the LUMO may have some extra weight within the backbone due to conjugation with the C_{60}, which could also contribute to the higher transmission at the Fermi level. To examine this possibility we have projected the density of states (DOS) onto the carbon atoms adjacent to the Fl rings of both molecules (projected density of states, PDOS, red atoms in Figure 3a). In Figure 4 we can see that in a region of ±0.5 eV above and below the Fermi level the DOS on this particular atom is significantly higher for **6** than for **4**.

To demonstrate that this enhanced DOS is expected to be reflected in the electronic communication of the molecules, we have analyzed a simple model, depicted in Figure 5a. In this model, the leads are represented by semi-infinite 1D chains with on-site energies ε_0, while the molecular groups are represented by a scattering region of five sites, with C_{60} groups represented by onsite energies ε_1, Fl units represented by ε_3 and the carbon atoms connecting them represented by ε_2. The coupling strengths between adjacent sites are represented by the parameters α, β, γ, and δ as shown in Figure 5a.

After analytically calculating a formula for both the transmission of the system and the DOS on this connecting site (for details, see the Supporting Information and ref 28), we fit the model parameters to the DFT transport results of the **6** cis case. Due to the simplicity of the model, the main aim of the fit was to obtain good agreement around the Fermi energy which, as can be seen in Figure 5b, was indeed achieved. As a further step, the analytical formula for the transmission was fitted to the **4** cis DFT transport results, but this time with only one fitting parameter, namely the on-site energy of the connecting site (ε_2). The remaining parameters were taken from the previous fit. As a result of this process, we obtained an $\varepsilon_2 = 2.8$ for compound **4** and $\varepsilon_2 = 1.53$ for compound **6**, which adequately reproduces the lower transmission of **4** compared to **6**. With the fitted parameters, the DOS on the connecting site was calculated, and the results for both transmission and DOS are displayed in parts b and c of Figure 5, respectively. We can see that the model

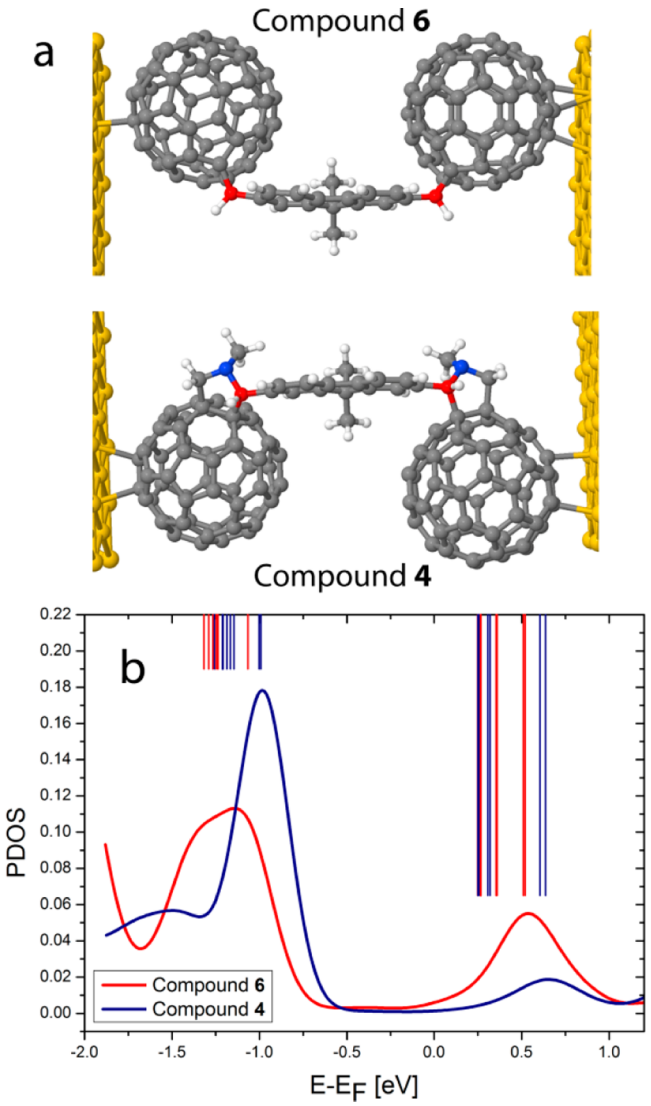

Figure 4. (a) Red atoms show the carbon atoms for which we have projected the DOS onto (blue atoms represent nitrogen, gray atoms represent carbon). (b) Density of states projected onto the atoms connecting the C_{60}s to the Fl backbone (red atoms in (a)). Compound **6** is described by the red line; compound **4** is described by the blue line. The vertical lines are the previously calculated HOMO and LUMO levels.

does indeed capture the lower transmission of compound **4**, along with a reduced DOS on the connecting C atom site as expected. This supports our statement that the LUMO of **6** extends further into the backbone, contributing to the higher conductance compared to **4**.

Cyclic Voltammetry. The redox properties of **4** and **6**, along with those of C_{60}, were studied by cyclic voltammetry at room temperature in *o*-dichlorobenzene/acetonitrile (4:1) as solvent (Figure 6). The half-wave values for the first three redox processes are also presented in Table 1. Common to the electrochemical features of all the dumbbell-type molecules investigated here is the presence of three quasi-reversible reduction waves, which correspond to the first three reduction steps of the fullerene moiety (for **4** and **6** each wave corresponds to a two-electron process).

As expected, these reduction values are cathodically shifted compared with the parent C_{60}, a consequence stemming from the

dx.doi.org/10.1021/jo500342x | J. Org. Chem. 2014, 79, 4871−4877

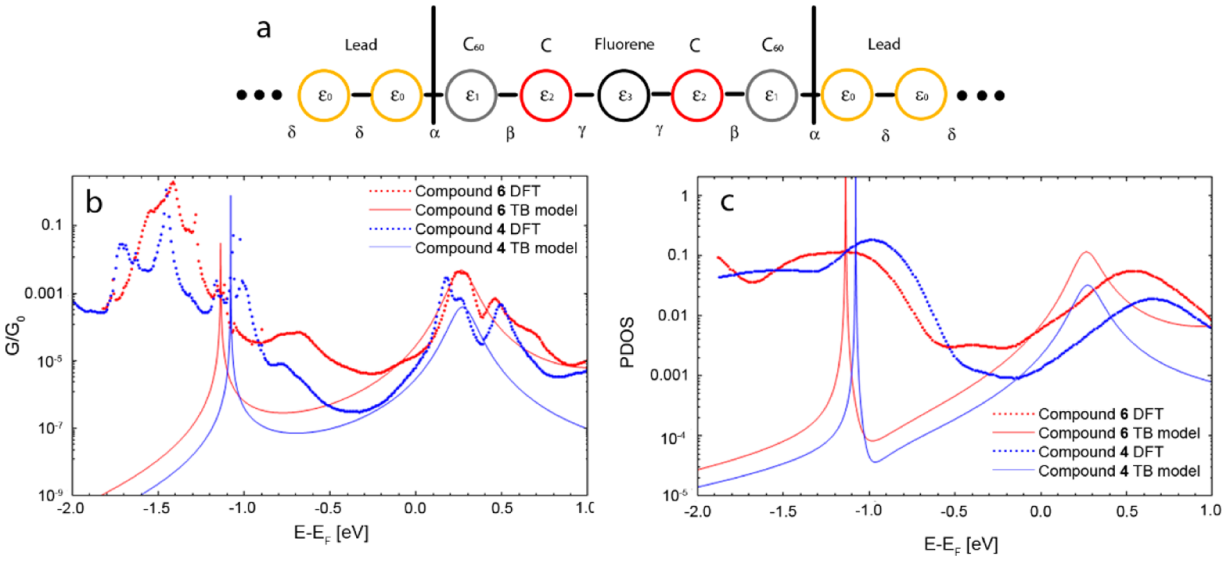

Figure 5. (a) Simple tight binding (TB) model of the dumbbell system. The fitted parameters are $\varepsilon_0 = 0$, $\varepsilon_1 = 0.27$, $\varepsilon_2 = 1.53$, $\varepsilon_3 = -0.95$, $\alpha = 0.49$, $\beta = 0.17$, $\gamma = 0.49$, $\delta = 3$ for 6 (Cp), while ε_2 =2.8 for 4 (Py). (b) DFT (thick lines with dots) and fitted (thin continuous lines) transmission curves. The red curves are for **6** (Cp), while the blue curves are for **4** (Py). (c) DFT (thick lines) and fitted (thin lines) PDOS curves onto the atom/site connecting the C_{60}s to the Fl. The red curves are for **6**, while the blue curves are for **4**.

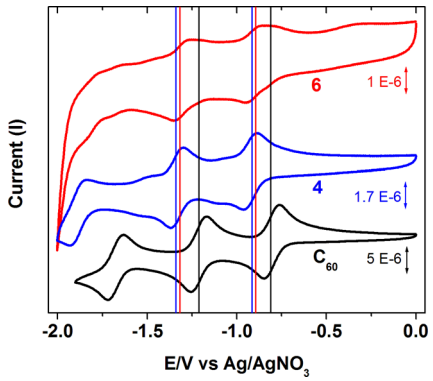

Figure 6. Cyclic voltammograms of compounds C_{60} (black), **4** (blue), and **6** (red) dissolved in *o*-DCB/MeCN (4:1 v/v). The voltage (V) is referenced to a $Ag/AgNO_3$ reference electrode (which was calibrated using an internal Fc/Fc^+ redox couple). Working electrode: GCE; counter electrode: Pt; supporting electrolyte: 0.1 M nBu_4NClO_4; scan rate: 100 mVs^{-1}. The vertical lines mark the first two half-wave positions for each compound.

Table 1. Cyclic Voltammetry Half-Wave Values of Compounds C_{60}, 4, and 6 vs $Ag/AgNO_3$[a]

compd	E^1_{red} (V)	E^2_{red} (V)	E^3_{red} (V)	E_{LUMO} (eV)
6	−0.90	−1.31	−1.84	−4.20
4	−0.92	−1.33		−4.18
C_{60}	−0.80	−1.21	−1.68	−4.30

[a]The approximate LUMO values are calculated from E^1_{red} on the basis of the oxidation potential of ferrocene in vacuum being −4.8 eV.

saturation of one of the double bonds of the buckyball, which consequently raises the LUMO energy.[29−31] In comparison with pristine C_{60}, overall conjugation has thus been reduced. Interestingly, however, the dumbbell-type molecule **6**, bearing the fused-cyclopropane rings shows consistently slightly lower values (by about 20 mV) for the first two reduction potentials. This suggests that compound **6** possesses greater electronic delocalization than **4** as a result of better preservation of the original C_{60} structure, as predicted in the previous section.

We can relate these values to the calculated energy differences of the LUMO levels shown in Figure 3. The trend in reduction potential between the pristine C_{60} and the dumbbell compounds in the CV measurements is maintained in the calculations for the lowest LUMO energies inside the junction. We have estimated the LUMO energies obtain by CV from their values relative to an internal reference, ferrocene (−4.8 eV). The relative energy differences noted in Table 1 agree very well with the theoretically predicted values in Figure 3, with the largest difference being between C_{60} and compounds **4** and **6** (roughly 100 meV), and a much smaller difference between the two dumbbells. Considering also that the image charge effects on the electrodes can be assumed to be the same for all three molecules (which is reasonable since in all three cases the buckyballs are lying closest to the electrodes), the ordering of the LUMO energies of the molecules when inside the junction can be directly compared to the ordering of the peaks in CV measurements, in which the molecules are not bound to an electrode, but rather in solution. The similarity in the ordering of the LUMO levels from the CV data and the calculations shows that upon inclusion between the two gold electrodes, the molecules will preserve their electronic properties. This is very useful for the tailoring of molecular properties inside molecular junctions.

UV−vis Spectra. Next, we turned to the electronic spectra of the molecules **4** and **6**, displayed in Figure 7, which show subtle, but important, differences. The spectra have been normalized to an absorbance of **1** at the peak maxima assigned to the fullerene $\pi-\pi^*$ transition.

Both molecules show a characteristic peak close to 430 nm, demonstrating the presence of functionalized C_{60}. The short red shift from the typical peak at 408 nm for pristine C_{60} (ascribed to the $\pi-\pi^*$ transition localized on C_{60})[32] is explained by the saturation of one of the double bonds on both C_{60} units. Compound **6** shows a slight broad band at around 500 nm, which differs from that observed for **4**; however, the assignment of optical transitions in this region is known to be difficult.[32]

dx.doi.org/10.1021/jo500342x | J. Org. Chem. 2014, 79, 4871−4877

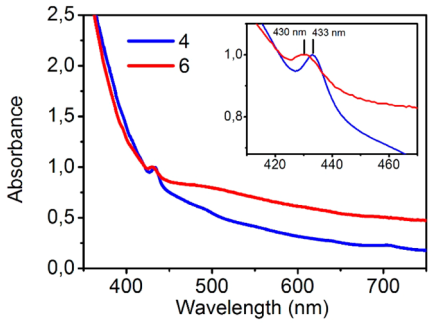

Figure 7. UV−vis spectra of compounds **4** (blue) and **6** (red) in toluene. The concentration used was 1×10^{-5} M. Inset shows a magnification of the 430 nm region showing the slightly shorter wavelength absorption of **6** versus **4**.

Hence, due to the lack of a clear band in the visible region of the spectra, no direct evidence of a feasible electron transfer along the molecules is present in the ground state. A closer inspection of the peaks for both compounds, however, reveals a slightly lower redshift relative to pristine C_{60} for compound **6** (430 nm) compared with compound **4** (432 nm). This follows with the idea that the Cp group preserves the original π system of the fullerene better than the Py, which in turn produces more of an alternating double−single bonding pattern (with the Cp unit counting as a double bond). The UV−vis spectra are fully consistent with the theoretical calculations and support the idea that the Cp groups provide the better electronic communication.

These results are also in qualitative agreement with a study performed by Kim et al. on a set of carbazole-functionalized fullerenes, where the relative changes in the reductions peaks are similar.[33] Interestingly, it was noted in this study that the reduction value of the compound containing the Py connection was anodically shifted with respect to PCBM (which also contains a Cp group) by several tens of millivolts. This can be explained by the strong donor property of the carbazole group, which raises the level of the C_{60} localized LUMO. This demonstrates the sensitivity of the LUMO to the nature of the addend.

CONCLUSIONS

The synthesis and full characterization of the dumbbell molecules **4** (pyrrolidine) and **6** (cyclopropane) have been carried out. Theoretical calculations predict that the electronic communication through the cyclopropane group is enhanced with respect to the pyrrolidine. First, the single molecule conductance values when wired between two gold electrodes were calculated to follow the order C_{60} (0.4 G_0) ≫ cyclopropane dumbbell **6** (1.5×10^{-5} G_0) > pyrrolidine dumbbell **4** (6×10^{-6} G_0). We found that dumbbell **6** has energetically the lowest lying LUMO level inside the junction in comparison with **4**, although the LUMO of C_{60} is still lower. By projecting the density of states onto the carbon atoms adjoining the fluorene and the C_{60} groups for both dumbbells, we found a greater weight of the LUMO at this site on the cyclopropane dumbbell **6**. This indicates that the LUMO is more delocalized within the molecule, which further contributes to the improved communication. The UV−vis spectra and cyclic voltammetry properties of both dumbbells have been measured. A smaller red-shift of the fullerene $\pi-\pi^*$ transition was found for dumbbell **6**, suggesting it to be closer in structure to pristine C_{60}. Also, slightly less negative reduction potentials were found for **6** by cyclic voltammetry, which points toward the same conclusion and is in full agreement with our calculations. The combined theory and experimental results show that electronic communication in the cyclopropane dumbbell is more efficient than in the pyrrolidine analogue with fully saturated bonds. This work strengthens the idea that overall the cyclopropane group behaves in a quasi-double bond manner.

EXPERIMENTAL SECTION

Chemicals. All reagents were purchased commercially and were used without further purification. All solvents used were synthetic grade. Purification of the products was carried out by flash silica gel chromatography with silica gel 60, 0.04−0.06 mm (230−400 mesh ASTM).

The synthetic strategy followed for the preparation of both dumbbell-type molecules is based on the known reactivity of fullerenes with 1,3-dipoles, which yields the respective cycloadducts.[34,35] As presented in Scheme 1, compound **3** was obtained in two synthetic steps from commercially available dibromofluorene (**1**). Compound **4** was then synthesized following a similar experimental procedure followed for related molecules,[18] involving a 2-fold Prato reaction[36] from the dialdehyde (**3**) and sarcosine (*N*-methylglycine) in the presence of C_{60}, by refluxing in toluene for 4 h. The synthesis of compound **6** has been described previously.[19]

Synthesis of Compound 4. 2,7-Dialdehyde-9,9′-dioctylfluorene (compound **3**) (200 mg, 0.448 mmol), sarcosine (318 mg, 3.582 mmol), and fullerene (2.58 g, 3.582 mmol) were dissolved into 80 mL of PhCl and heated at reflux temperature under Ar stream for 4 h. The reaction was quenched by warming to room temperature and washing with 3 × 100 mL of H_2O. The organic phase was collected, dried over $MgSO_4$, filtered, and concentrated to dryness. The crude material was then purified via silica gel chromatography. First CS_2 was used to remove the unreacted fullerene, and then dichloromethane was used for the recovery of the desired product. A brown solid was obtained (30 mg). Yield = 9%. ^{1}H NMR (CS_2 with internal reference $CDCl_3$, 700 MHz, 298 K): δ = 8.5−7.5 (bm, 6H), 5.27 (s, $2H_{pyrrolidine}$), 5.27 (d, J = 5.64 Hz, $2H_{pyrrolidine}$), 4.58 (d, J = 8.75 Hz, $2H_{pyrrolidine}$), 3.10 (s, 3H), 2.21 (bs, 4H), 1.7−1.0 (m, 30H). ^{13}C NMR (CS_2 with internal reference $CDCl_3$, 175 MHz, 298 K): δ = 156.5, 154.1, 153.7, 140.1, 137.3, 136.5, 84.4, 78.1, 70.8, 69.6, 55.8, 40.7, 33.1, 31.4, 30.8, 30.4, 30.6, 24.2, 23.1, 15.5 ppm. MS (MALDI-ToF): m/z 1942.404 (M + H), calcd mass for $C_{155}H_{52}N_2$ 1941.416.

ASSOCIATED CONTENT

Supporting Information

Chemical characterization data (^{1}H NMR, ^{13}C NMR MALDI-TOF mass spectrum). STM experiments and procedures. Theoretical details including details of molecular orbital calculations and formulas used in PDOS calculations. This material is available free of charge via the Internet at http://pubs.acs.org.

AUTHOR INFORMATION

Corresponding Authors

*E-mail: edmund.leary@imdea.org.

*E-mail: nazmar@quim.ucm.es.

Author Contributions

⊥A.L.R., K.G., E.L., and C.E. contributed equally.

Notes

The authors declare no competing financial interest.

ACKNOWLEDGMENTS

Financial support was provided by the Ministerio de Economía y Competitividad (MINECO) of Spain (CTQ2011-24652, PIB2010JP-00196, MAT2011-25046, RYC-2008-03328 and CSD2007-00010 projects) and the Comunidad de Madrid program *Nanobiomagnet* S2009/MAT-1726. S.F. acknowledges MINECO and ESF for an R&C grant, and the CAM

(MADRISOLAR-2 project S2009/PPQ-1533) is acknowledged. This work has also been supported by the ERC (AdGChirallcarbon ERC-2012-ADG_20120216). We also acknowledge support by the UK EPSRC and the European Union (FP7) through programs ITN "FUNMOLS" (Project No. 212942), ITN "NANOCTM", ELFOS (FP7-ICT2009-6), and "MOLESCO" (Project No. 606728). C.E. acknowledges funding from the A.G. Leventis Foundation.

REFERENCES

(1) Guldi, D. M.; Martin, N. M. *Fullerenes: From Synthesis to Optoelectronic Properties*; Kluver Academic Publishers: Dordrecht, 2002.
(2) Hirsch, A.; Bettreich, M. *Fullerenes, Chemistry and Reactions*; Wiley-VCH: Weinheim, 2005.
(3) Langa, F.; Nierengarten, J. F. *Fullerenes: Principles and Applications*, 2nd ed., RSC: Cambridge, 2012.
(4) Martin, N.; Sanchez, L.; Illescas, B.; Perez, I. *Chem. Rev.* **1998**, *98*, 2527−2547.
(5) Martin, N.; Sanchez, L.; Herranz, M. A.; Illescas, B.; Guldi, D. M. *Acc. Chem. Res.* **2007**, *40*, 1015−1024.
(6) Guldi, D. M.; Illescas, B. M.; Ma Atienza, C.; Wielopolskia, M.; Martin, N. *Chem. Soc. Rev.* **2009**, *38*, 1587−1597.
(7) Luis Delgado, J.; Bouit, P.-A.; Filippone, S.; Angeles Herranz, M.; Martin, N. *Chem. Commun.* **2010**, *46*, 4853−4865.
(8) Dennler, G.; Scharber, M. C.; Brabec, C. J. *Adv. Mater.* **2009**, *21*, 1323−1338.
(9) Kippelen, B.; Bredas, J.-L. *Energy Environ. Sci.* **2009**, *2*, 251−261.
(10) Thompson, B. C.; Frechet, J. M. J. *Angew. Chem., Int. Ed.* **2008**, *47*, 58−77.
(11) Guenes, S.; Neugebauer, H.; Sariciftci, N. S. *Chem. Rev.* **2007**, *107*, 1324−1338.
(12) Martin, N. *Chem. Soc. Rev.* **2006**, 2093−2104.
(13) Eiermann, M.; Haddon, R.; Knight, B.; Li, Q.; Maggini, M.; Martin, N.; Ohno, T.; Prato, M.; Suzuki, T.; Wudl, F. *Angew. Chem., Int. Ed.* **1995**, *34*, 1591−1594.
(14) Ohno, T.; Martin, N.; Knight, B.; Wudl, F.; Suzuki, T.; Yu, H. *J. Org. Chem.* **1996**, *61*, 1306−1309.
(15) Knight, B.; Martin, N.; Ohno, T.; Orti, E.; Rovira, C.; Veciana, J.; VidalGancedo, J.; Viruela, P.; Viruela, R.; Wudl, F. *J. Am. Chem. Soc.* **1997**, *119*, 9871−9882.
(16) Kooistra, F. B.; Leuning, T. M.; Martinez, E. M.; Hummelen, J. C. *Chem. Commun.* **2010**, *46*, 2097−2099.
(17) Xiao, Z.; Ye, G.; Liu, Y.; Chen, S.; Peng, Q.; Zuo, Q.; Ding, L. *Angew. Chem., Int. Ed.* **2012**, *51*, 9038−9041.
(18) Leary, E.; Teresa Gonzalez, M.; van der Pol, C.; Bryce, M. R.; Filippone, S.; Martin, N.; Rubio-Bollinger, G.; Agrait, N. *Nano Lett.* **2011**, *11*, 2236−2241.
(19) Gillemot, K.; Evangeli, C.; Leary, E.; La Rosa, A.; González, M. T.; Filippone, S.; Grace, I.; Rubio-Bollinger, G.; Ferrer, J.; Martín, N.; Lambert, C. J.; Agraït, N. *Small* **2013**, *9*, 3812−3822.
(20) Wiberg, K. *Acc. Chem. Res.* **1996**, *29*, 229−234.
(21) Anslyn, E. V; Dougherty, D. A. *Modern Physical Organic Chemistry*; University Science Books: Sausalito, CA, 2006.
(22) Soler, J.; Artacho, E.; Gale, J.; Garcia, A.; Junquera, J.; Ordejon, P.; Sanchez-Portal, D. *J. Phys.: Condens. Matter* **2002**, *14*, 2745−2779.
(23) Perdew, J.; Zunger, A. *Phys. Rev. B* **1981**, *23*, 5048−5079.
(24) Troullier, N.; Martins, J. *Phys. Rev. B* **1991**, *43*, 8861−8869.
(25) Rocha, A.; Garcia-Suarez, V.; Bailey, S.; Lambert, C.; Ferrer, J.; Sanvito, S. *Phys. Rev. B* **2006**, *73*, 085414.
(26) Rocha, A.; Garcia-Suarez, V.; Bailey, S.; Lambert, C.; Ferrer, J.; Sanvito, S. *Nat. Mater.* **2005**, *4*, 335−339.
(27) Markussen, T.; Settnes, M.; Thygesen, K. S. *J. Chem. Phys.* **2011**, *135*, 144104.
(28) Sparks, R. E.; Garcia-Suarez, V. M.; Manrique, D. Z.; Lambert, C. J. *Phys. Rev. B* **2011**, *83*, 075437.
(29) Suzuki, T.; Maruyama, Y.; Akasaka, T.; Ando, W.; Kobayashi, K.; Nagase, S. *J. Am. Chem. Soc.* **1994**, *116*, 1359−1363.
(30) Chlistunoff, J.; Cliffel, D.; Bard, A. J. *Handbook of Organic Conductive Molecules and Polymers*; John Wiley & Sons: New York, 1997.
(31) Echegoyen, L.; Echegoyen, L. *Acc. Chem. Res.* **1998**, *31*, 593−601.
(32) Thomas, K.; Biju, V.; Guldi, D.; Kamat, P.; George, M. *J. Phys. Chem. B* **1999**, *103*, 8864−8869.
(33) Kim, H. U.; Mi, D.; Kim, J.-H.; Park, J. B.; Yoon, S. C.; Yoon, U. C.; Hwang, D.-H. *Sol. Energy Mater. Sol C* **2012**, *105*, 6−14.
(34) Segura, J.; Martin, N. *Chem. Soc. Rev.* **2000**, *29*, 13−25.
(35) Segura, J.; Martin, N.; Guldi, D. *Chem. Soc. Rev.* **2005**, *34*, 31−47.
(36) Prato, M.; Maggini, M. *Acc. Chem. Res.* **1998**, *31*, 519−526.